DOI: 10.1002/ejic.200600495

Synthesis and Characterization of Some New 22-Membered Chalcogenoaza Macrocycles and Their Co^{II} and Ni^{II} Complexes

Upali Patel,[a] Harkesh B. Singh,*[a] and Ray J. Butcher[b]

Keywords: Cobalt / Magnetic properties / N ligands / Selenium / Tellurium

The [2+2] cyclocondensation of bis(*o*-formylphenyl)chalcogenides (**9**, **10**) with *trans*-1,2-diaminocyclohexane affords novel macrocyclic ligands **11** and **12** in very good yields. Crystals of **11** are triclinic, space group $P\bar{1}$ with a = 11.4037(11), b = 11.8184(12), c = 14.6835(14) Å, Z = 4 and those of **12** are triclinic, space group $P\bar{1}$ with a = 11.2692(9), b = 12.8612(11), c = 15.2439(12) Å and Z = 2. Reduction of **11** with sodium borohydride affords macrocycle **13**. The coordination chemistry of **11** has been studied with the "hard" metal ions Ni^{II} and Co^{II}. Reaction of $NiCl_2{\cdot}6H_2O$ with one molar equivalent of **11** in refluxing methanol followed by addition of NH_4PF_6 affords Ni^{II} complex **14**. The assignment of an octahedral geometry to **14** follows from its paramagnetism (μ_{eff} = 2.50 μ_B) and UV/Vis spectrum and was further confirmed by single-crystal X-ray diffraction studies. The crystal structure of **14** consists of a distorted octahedral nickel center coordinated by two selenium and four nitrogen atoms. Complex **14**: hexagonal, space group $P6_1$, a = 17.0747(16), b = 17.0747(16), c = 29.958(4) Å, Z = 6. Co^{II} complexes **15** and **16** of selenaaza macrocycles were prepared by the reaction of $Co(ClO_4)_2{\cdot}6H_2O$ with **11** and **3**, respectively. Complex **16**: monoclinic, space group C_2, a = 17.160(2), b = 10.9660(14), c = 9.4941(12) Å, Z = 2. The cyclic voltammograms of **15** and **16** in MeCN solution show well-behaved quasi-reversible couples.

Introduction

Over the last decade mixed-donor chalcogen (N, O, S, Se, Te) macrocycles have attracted considerable attention.[1–7] Among them, the chalcogenoaza macrocycles containing heavier chalcogens (Se, Te) have been less studied. Our group has been involved in the synthesis and complexation studies of Schiff base selenaaza and telluraaza macrocycles **1**–**5**.[6,7] Interestingly, Schiff base macrocycle **2** shows a tendency to undergo transmetalation with Pt^{II} and Hg^{II} cations,[6a] and **1** hydrolyzed with Pd^{II} cation leads to cleavage of the macrocycle.[6b] Macrocycles **5** and **6** exhibit contrasting ligating behavior with Pd^{II} and Pt^{II}. Thus, macrocycle **5** forms a 23-membered metallamacrocycle on ligation with Pt^{II} where oxidative addition of the C–Se bond to the Pt^{II} center occurs to form a hexacoordinate Pt^{IV} complex.[7c] The synthesis and structure of complexes of Hg_2^{2+} and Pb^{II} with 28-membered selenaaza macrocycle **4** have also been reported.[7d] There are limited examples of Ni^{II} complexes of mixed-donor selenaaza macrocycles,[7b,7e] and there are no reports on the structures of Co^{II} complexes of selenaethers or selenaaza macrocycles in the literature. However, two examples of structurally characterized Co^{III} complexes of selenamacrocycles have been reported. The Co^{III} complex of sarcophagine theme, with an N3Se3 donor (**7**), has been obtained from the reaction of $CoCl_3$ with $\{MeC[CH_2Se(CH_2)_2{-}NH_2]_3\}$ in HCHO and $MeNO_2$.[5] The complex $[CoX_2([16]aneSe_4)]PF_6$ (X = Br) (**8**) has been prepared by the reaction of CoX_2 (X = Cl, Br, I) with $[16aneSe_4]$ and NH_4PF_6, where the original Co^{II} has been oxidized to Co^{III}.[8] Here we report the synthesis and characterization of some new 22-membered selenaaza and telluraaza macrocycles derived from *trans*-1,2-diaminocyclohex-

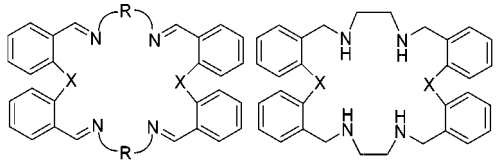

1: X = Se, R = -CH_2CH_2-
2: X = Te, R = -CH_2CH_2-
3: X = Se, R = -$CH_2CH_2CH_2$-
4: X = Se, R = -CH_2CH_2-N-CH_2CH_2-

5: X = Se
6: X = Te

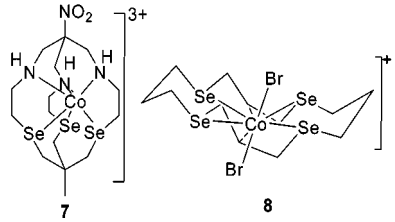

7 **8**

[a] Department of Chemistry, Indian Institute of Technology Bombay,
Mumbai, 400 076, India
Fax: +91-22-2572-3480
E-mail: chhbsia@chem.iitb.ac.in
[b] Department of Chemistry, Howard University,
Washington, DC 20059, USA

ane, which imposes some rigidity on the macrocycle ring, and the coordination properties of the selenaaza macrocycles towards Co^{II} and Ni^{II}. Although we have earlier reported the synthesis of a Co^{II} complex with **1**, our attempts to characterize the complex by single crystal structure determination were unsuccessful.[7b] Now we report the first X-ray structural characterization of a Co^{II} complex with a selenaaza macrocycle and its detailed magnetic properties. The coordination behavior of the telluraaza macrocycles with Pd^{II} is also studied.

Results and Discussion

Compounds **3**,[7b] **9**,[7a] and **10**[6a] were synthesized by the reported procedures. Ligands **11** and **12** were obtained in good yield by the stoichiometric reaction of bis(*o*-formylphenyl) chalcogenides **9** and **10** with *trans*-1,2-diaminocyclohexane as white and yellow solids, respectively (Scheme 1). Reduction of Schiff-base ligand **11** with an excess amount of sodium borohydride in ethanol afforded tetraamino derivative **13** as a white solid in good yield (Scheme 1). All these ligands were characterized by elemental analysis, IR-, ^{1}H-, ^{13}C-, and ^{77}Se/^{125}Te NMR spectroscopy, and ESI mass spectrometry. Both of the Schiff-base ligands (**11**, **12**) were also characterized by single-crystal X-ray crystallography.

For ligand **11**, broadening of the ^{1}H- and ^{13}C NMR signals was observed at room temperature; hence the spectra were recorded at –50 °C. There were no significant changes in the ^{1}H NMR spectrum even at –50 °C. However, the ^{13}C NMR spectrum shows two sets of well-resolved peaks at low temperature, which may be due to the fluxional behavior of **11**.

The observation of single signals in the ^{77}Se NMR spectra of the macrocycles **11** and **13** confirmed the equivalence of the selenium atoms. The ^{77}Se NMR signals are observed at δ = 404 and 340 ppm for **11** and **13**, respectively. These values are comparable to the corresponding values for 22-membered selenaaza Schiff base **1** and reduced derivative **5**.[7b] Ligand **12** exhibits the ^{125}Te NMR signal at δ = 581 ppm.

Crystal Structures of 11 and 12

An ORTEP view of **11** is shown in Figure 1 and selected bond lengths and angles are listed in Table 1. The compound crystallizes in the triclinic crystal system with the space group $P\bar{1}$. N1A and N2A are intramolecularly coordinated to Se1 and Se2, respectively, making the geometry around selenium T-shaped. The Se1···N1A and Se2···N2A bond lengths (2.816 and 2.782 Å, respectively) are only slightly longer than the Se···N distance observed for 22-membered selenaaza macrocycles **1** and **5**[7b,7e] (2.723 and 2.729 Å, respectively). The Se1···N1B and Se2···N2B the distances (4.409 and 4.322 Å, respectively) are longer than the sum of the van der Waals radii (3.5 Å) and indicate no intramolecular interaction. Surprisingly, the transannular Se···Se distance (5.881 Å) is longer than that in **1** (3.808 Å).[7b] The bond angles C1A–Se1–C1B and C20A–Se2–C20B are 97.79(13)° and 97.10(13)°, respectively, and are smaller than those of macrocycle **1** [100.2(3)°].

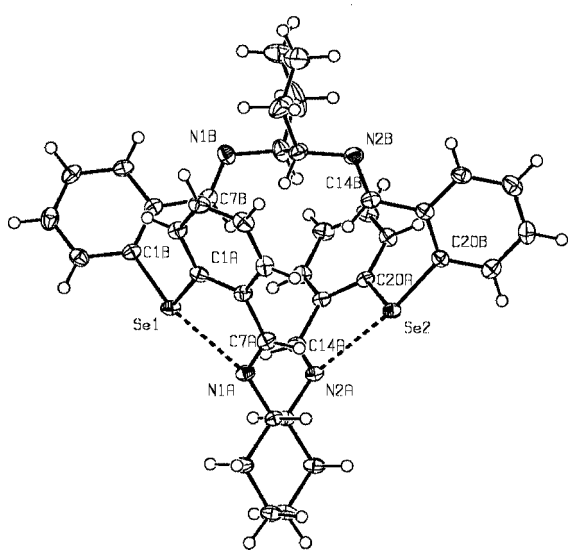

Figure 1. ORTEP diagram of **11**.

An ORTEP view of compound **12** is represented in Figure 2 and selected bond lengths and angles are listed in Table 2. Similar to macrocycle **11**, only one of the nitrogen atoms is coordinated to each tellurium in **12**. The

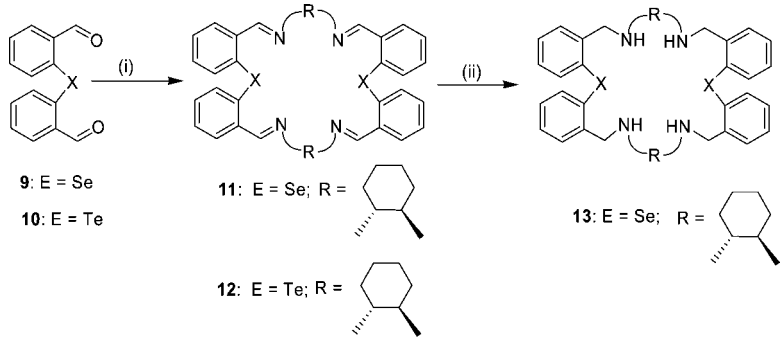

Scheme 1. Reagents: (i) *trans*-1,2-diaminocyclohexylamine, CH_3CN; (ii) $NaBH_4$, EtOH, reflux.

Table 1. Significant bond lengths [Å] and angles [°] for **11**.

Se1–C1A	1.917(3)	Se1–C1B	1.927(3)
Se2–C20A	1.921(3)	Se2–C20B	1.932(3)
N1A–C7A	1.259(4)	N2A–C14A	1.263(4)
C1A–Se1–C1B	97.79(13)	C20A–Se2–C20B	97.10(13)

Te2···N2B#2 and Te2#2···N2B bond lengths are 2.662 and 2.667 Å, respectively, and are similar to the Te···N bond length of 2.701 Å in **2**.[6a] The Te2#2···N1B#2 (4.707 Å) and Te2···N1B (4.708 Å) distances indicate no intramolecular interaction. The transannular Te···Te distance (4.904 Å) is comparable to that observed for the 22-membered telluraza macrocycle **2** (4.979 Å)[6a] and longer than the sum of the van der Waals radii (4 Å). The C1B–Te2–C20B#2 bond angle is 94.49°, which is comparable to that observed for telluraaza macrocycle **2**. The packing diagram shows hydrogen bonding between the macrocyclic N atom and the H of solvent dichloromethane.

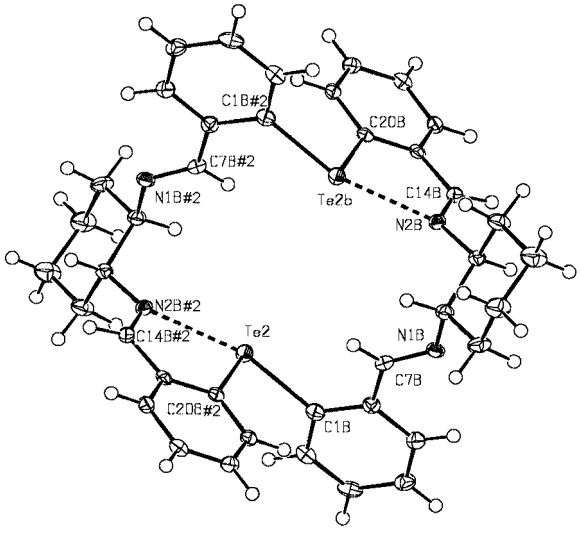

Figure 2. ORTEP diagram of **12**.

Table 2. Significant bond lengths [Å] and angles [°] for **12**.[a]

Te1–C1A	2.117(3)	Te2–C1B	2.166(3)
Te1–C20A#1	2.156(3)	Te2–C20B#2	2.109(2)
Te2–N1B	4.708	Te2#2–N2B	2.667
Te2–N2B#2	2.667	Te2#2–N1B#2	4.707
C1A–Te1–C20A#1	94.73(10)	C20B#2–Te2–C1B	94.49(9)

[a] Symmetry transformations: #1: $-x + 1, -y + 1, -z$; #2: $-x + 1, -y + 1, -z + 1$.

Complexation

With the objective of synthesizing metal complexes, macrocycles **11**, **3**, and **12** were treated with the transition metal ions Ni^{II}, Co^{II}, and Pd^{II} in a 1:1 molar ratio to afford complexes **14**, **15**, **16**, and **17**.

Complex 14

Refluxing equimolar amounts of ligand **11** and $NiCl_2·6H_2O$ in a 1:1 ratio and subsequent addition of ammonium hexafluorophosphate gave reddish-brown, air-stable complex **14** (Scheme 2). The IR spectrum of **14** shows the presence of the PF_6^- anion [ν(P–F) = 848, δ(F–P–F) = 565 cm^{-1}] and also displays the characteristic ν(C=N) stretching frequency at 1627 cm^{-1}, which is shifted slightly compared with the ν(C=N) of free ligand **11** (1642 cm^{-1}). The electronic spectrum (UV/Vis) of complex **14** was recorded at room temperature in CH_3CN. It shows four bands at 218 (12752), 348 (613), 450 (123) and 850 nm (50 $M^{-1}cm^{-1}$), which can be assigned to the intraligand π–π* and $^3A_{2g}\rightarrow{}^3T_{1g(P)}$, $^3A_{2g}\rightarrow{}^3T_{2g}$, and $^3A_{2g}\rightarrow{}^3T_{1g(F)}$ transitions, respectively.[9] The assignment of an octahedral geometry to complex **14** [Ni(**11**)]$(PF_6)_2$ follows from its paramagnetism (μ_{eff} = 2.50 μ_B), which indicates an $n = 2$, $S = 1$ high-spin complex with two unpaired electrons. This was further confirmed by single-crystal X-ray studies (vide infra). As expected for octahedral Ni^{II} complexes, complex **14** is ESR silent.[10,11]

The structure of **14** (Figure 3) shows that Ni^{II} occupies the macrocycle cavity and is bonded to all four nitrogen and two selenium donors to complete the distorted octahedral geometry [Ni–N2A = 2.052(5), Ni–N1B = 2.086(5), Ni–N1A = 2.059(5), Ni–N2B = 2.095(5), Ni–Se2 = 2.508(10), and Ni–Se1 = 2.510(10) Å; Table 3]. The average Ni–Se distance (2.509 Å) is comparable to the average Ni–Se distance (2.52 Å) observed for [Ni(**1**)]$(PF_6)_2$ but smaller than the average Ni–Se distances in [Ni(**3**)]$(PF_6)_2$[7b] (2.568 Å) and

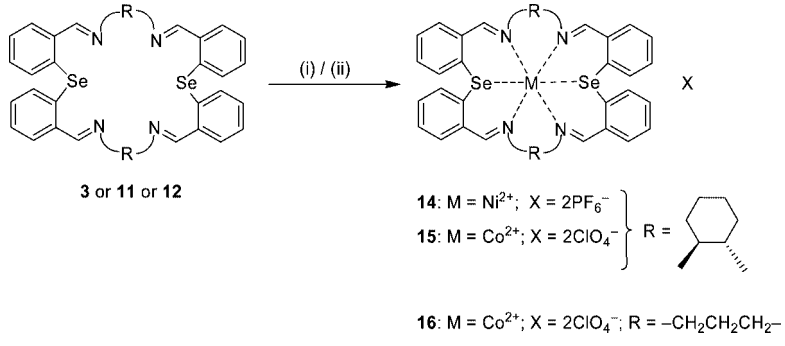

Scheme 2. Reagents: (i) $NiCl_2·6H_2O$, NH_4PF_6, MeOH; (ii) $Co(ClO_4)_2·6H_2O$, CH_3CN.

$[Ni(\mathbf{5})](PF_6)_2$ (2.618 Å).[7e] The C1A–Se1–C1B angle [98.3(3)°] differs slightly from that of the ligand (97.79°). The angles around the central metal atom lie in the range 77.8(2)–101.54(19)° for those involving mutually *cis* donor atoms and 165.22(14)–179.12(17)° for the mutually *trans* donor atoms, thereby deviating only slightly from those expected for a regular octahedral geometry.

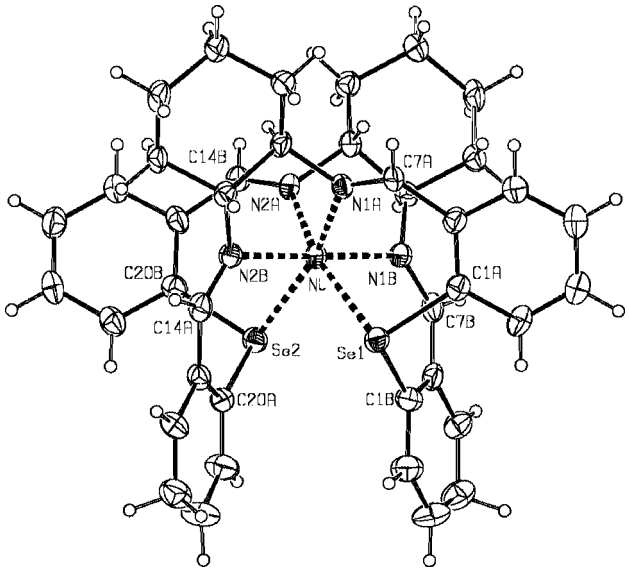

Figure 3. ORTEP diagram of **14** (PF_6 anion and H atoms have been omitted for clarity).

Table 3. Significant bond lengths [Å] and angles [°] for **14**.

Ni–N2A	2.052(5)	Ni–N1B	2.086(5)
Ni–N1A	2.059(5)	Ni–N2B	2.095(5)
Ni–Se2	2.5089(10)	Ni–Se1	2.5105(10)
Se1–C1B	1.909(7)	Se1–C1A	1.944(7)
Se2–C20B	1.923(7)	Se2–C20A	1.933(6)
N1A–C7A	1.275(8)	N2A–C14B	1.267(8)
C1B–Se1–C1A	98.3(3)	C20B–Se2–C20A	98.0(3)

Complex 15

The reaction of ligand **11** and $Co(ClO_4)_2{\cdot}6H_2O$ in a 1:1 ratio afforded brown complex **15**. Complex **15** is soluble in CH_3CN and acetone but decomposes in DMSO. The IR spectrum shows the ν(C=N) band shifted from 1642 to 1617 cm^{-1}, thus implying the coordination of all the imine nitrogens to the metal. The molecular ion peak is not observed in the ESI mass spectrum of the complex, although the peaks at m/z = 894 and 795 correspond to $[M - ClO_4]^+$ and $[M - 2ClO_4]^+$, respectively, and confirm the formation of complex **15**. The bands at 222 (15162) and 356 nm (1487) in the UV/Vis spectrum can be assigned to intraligand π–π* transitions and the band at around 546 nm (218) is due to the $^4T_{1g(F)} \rightarrow {}^4T_{1g(P)}$ transitions. The cyclic voltammogram in acetonitrile solution reveals a quasireversible wave at $E_{1/2}$ = 0.236 V versus saturated calomel electrode (SCE) with a ΔE value of 0.070 V.

Complex 16

Co^{II} complex **16** was synthesized similarly with a 1:1 ratio of ligand **3** and $Co(ClO_4)_2{\cdot}6H_2O$ in acetonitrile. This complex is also soluble in acetone and acetonitrile but decomposes in DMSO. The elemental analysis data of complex **16** suggest the formation of a 1:1 product. The IR spectroscopic measurements show that the ν(C=N) absorption of **16** has shifted from 1642 to 1627 cm^{-1}. In the ESI mass spectrum the highest recorded peak for complex **16** is found at m/z = 814 and can be assigned to $[\mathbf{16} - ClO_4]^+$,which confirms the formation of the complex. The cyclic voltammetric study shows a well-behaved, quasireversible redox wave with $E_{1/2}$ = 0.249 V versus saturated calomel electrode (SCE) and a ΔE value of 0.062 V. The UV/Vis spectrum of **16** consists of three bands at 224 (18141), 354 (1734), 546 nm (285) due to π–π* and d–d transitions. The structure was confirmed by X-ray crystallographic studies.

Selected bond lengths and angles are given in Table 4 and the ORTEP diagram is shown in Figure 4. The complex crystallizes in the triclinic system with space group C_2. The Co^{II} ion is bound to the hexadentate macrocycle **3** by two selenium donors and four nitrogen donors. The notable feature of this structure is the Co^{II}–Se intermolecular interaction: the Co^{II}–Se distances [Co–Se1 = 2.593(6), Co–Sea = 2.593(6) Å] are longer then the Co^{III}–Se distance (2.340 Å) observed in the structure of macrobicyclic cage $[CoL]^{3+}$ (L = 8-methyl-1-nitro-6,10,19-triselena-3,13,16-triazabicyclo-[6.6.6]icosane) (**7**).[5] The angles around the central metal atom lie in the range 84.22(9)–98.89(18)° for those involving mutually *cis* donor atoms and 171.12(9)–174.6(2)° for those mutually *trans* donor atoms. Thus, they do not deviate greatly from the values of 90° and 180° expected for a regular octahedron. The Co–N bond lengths are Co–N1 = 2.128(3), Co–N1#1 = 2.129(3), Co–N2#1 = 2.157(3), and Co–N2 = 2.157(3) Å. The Se–C distances [Se–C17#1 = 1.927(4), Se–C1 = 1.928(3), C17–Se#1 = 1.927(4) Å] are comparable to the parent ligand and are close to the sum of the Pauling covalent radii for selenium (1.17 Å) and an sp^2-hybridized carbon (0.74 Å). The C–Se–C angle [C17#1–Se–C1 = 96.56(15)°, C17#1–Se–C = 97.44(11)°] deviate slightly from the C–Se–C angle (97.44°) in the ligand.

Table 4. Significant bond lengths [Å] and angles [°] for **16**.

Co–N1	2.128(3)	Co–N1#1	2.129(3)
Co–N1#1	2.129(3)	Co–N2#1	2.157(3)
Co–N2	2.157(3)	C17–Se#1	1.927(4)
Co–Se	2.5931(6)	Co–Se#1	2.5931(6)
Se–C17#1	1.927(4)	Se–C1	1.928(3)
N1–C7	1.290(5)	N2–C11	1.262(6)
C17#1–Se–C1	96.56(15)		

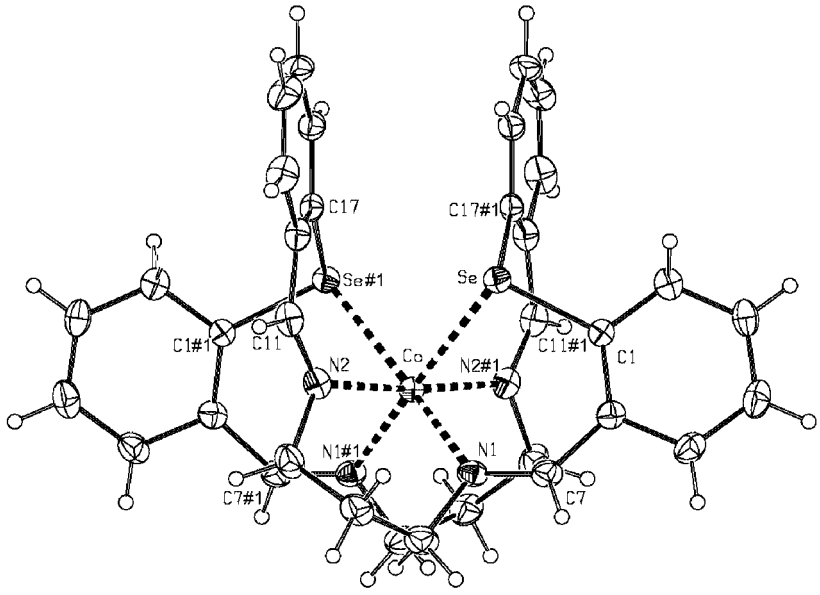

Figure 4. ORTEP diagram of **16** (ClO_4 has been omitted for clarity).

Complex 17

The reaction of **12** with $[PdCl_2(C_6H_5CN)_2]$ followed by the addition of an excess amount of ammonium hexafluorophosphate afforded yellow complex **17** (Scheme 3). The elemental analysis data suggest the formation of a 1:1 ligand/metal complex. The ^1H NMR spectrum exhibits two sets of signals for each kind of proton. Two singlets at δ = 8.5 and 9.0 ppm are observed for the imine protons, with one singlet being shifted downfield from δ = 8.5 ppm (for the parent imine proton) to δ = 9.0 ppm. The N-C*H*-CH_2 protons also appear as two singlets, with one of these singlets being shifted downfield relative to the parent compound. The ^{13}C NMR spectrum also shows two sets of signal. The ^{125}Te NMR signal of complex **17** at δ = 751 ppm is shifted downfield relative to the parent compound (δ = 581 ppm), which indicates that tellurium is coordinated to the palladium. All NMR spectroscopic data confirm the coordination of the two imine nitrogens and two telluriums to palladium to form a square-planar geometry around it,[6c] which explains the two sets of signals, one for the coordinated part and another for the uncoordinated part. In the ESI mass spectrum the peaks at *m*/*z* = 934 and 1085 correspond to $[M - 2PF_6]^+$ and $[M - PF_6]^+$ and confirm the formation of complex **17**.

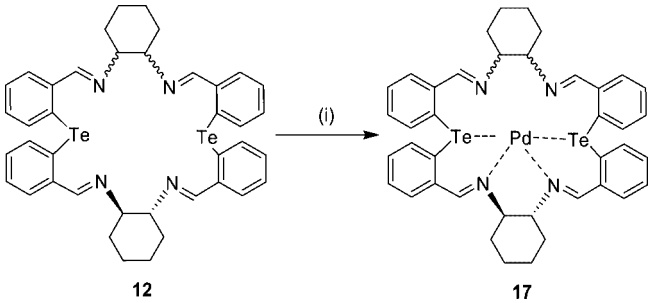

Scheme 3. Reagents: (i) $[PdCl_2(C_6H_5CN)_2]$, $CHCl_3/CH_2Cl_2$.

Magnetic Properties and ESR Data of 15 and 16

The thermal dependence of the molar magnetic susceptibility (χ_M) vs. *T* plot and the μ_{eff} vs. *T* plot are shown in the Figure 5. The molar magnetic susceptibility (χ_M) increases with a decrease in temperature, as expected for normal paramagnetic samples. The magnetic moment measurement in the temperature range 4 K (μ_{eff} = 1.3 μ_B) to 300 K (μ_{eff} = 2.3 μ_B) implies that compound **15** is a low-spin Co^{II} complex ($t_{2g}^6 e_g^1$) with one unpaired electron.

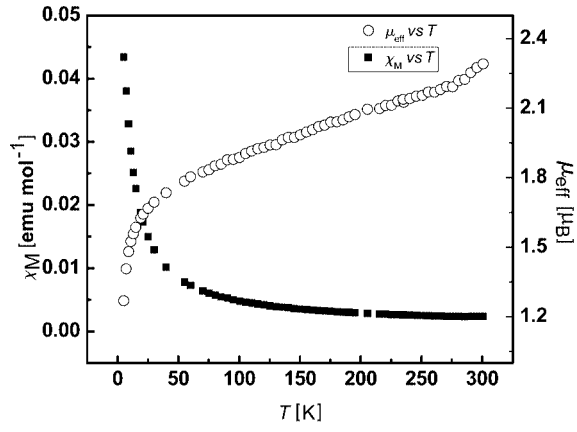

Figure 5. Magnetic properties of **15**: χ_M vs. *T* plot and μ_{eff} vs. *T* plot.

The distinct axial-type EPR spectrum of complex **15** is shown in Figure 6 ($g_1 = g_2 = 2.19$, $g_3 = 2.03$). The complex does not show a clear EPR signal at 298 K, which may be due to spin-lattice relaxation of the Co^{II} ion in an octahedral field at room temperature.[12] However, the signal starts developing from 268 K downwards (shown in Figure 6). The hyperfine splitting due to ^{57}Co (I = 5/2) is not seen even at 77 K.

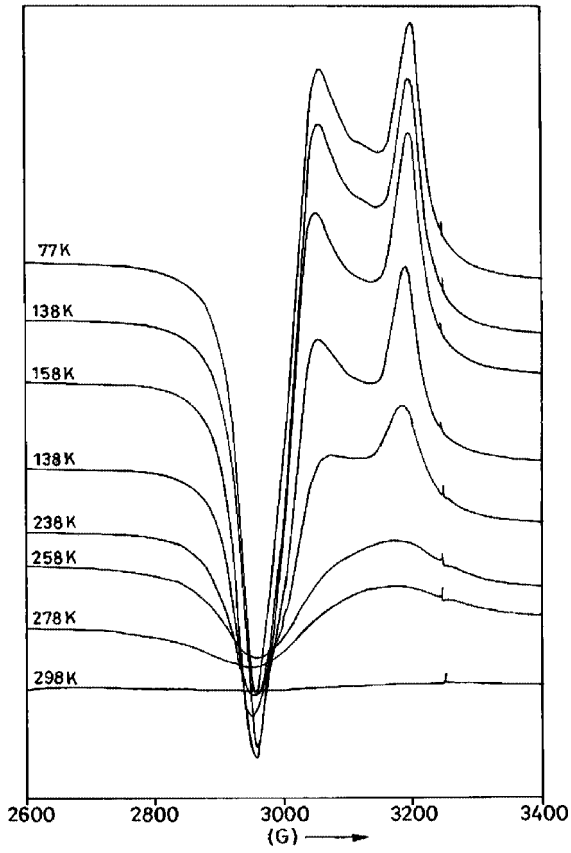

Figure 6. ESR spectra of **15** at variable temperature.

The variable-temperature magnetic susceptibility measurements for **16** were performed on powdered samples between 4 and 300 K. The χ_M vs. T and μ_{eff} = 2.84 $(\chi_M T)^{1/2}$ vs. T plots are shown in Figure 7. The molar magnetic susceptibility (χ_M) of **16** increases with a decrease in temperature, as expected for normal paramagnetic samples. The magnetic moment of **16** shows an μ_{eff} value ranging from 4.0 to 4.9 μ_B, which is higher than that expected for high-spin Co^{II} ($t_{2g}^4 e_g^2$) with three unpaired electrons (μ_s = 3.8 μ_B) and indicates the presence of an orbital contribution. However, these values are in good agreement with those observed for Co^{II} ions in a distorted octahedral arrangement.

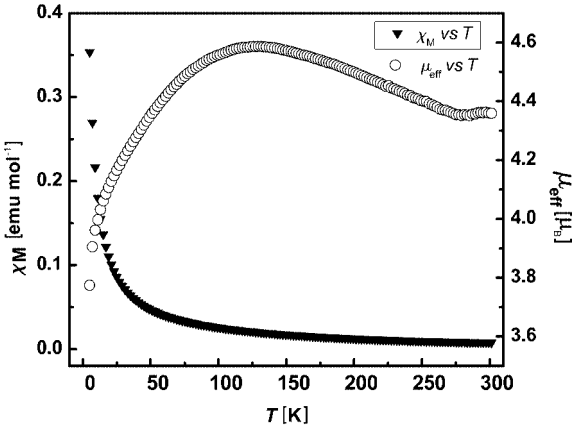

Figure 7. Magnetic properties of **16**: χ_M vs. T plot and μ_{eff} vs. T plot.

The complex does not show any EPR signal at 298 K, which may be due to spin lattice relaxation.[12] However, it starts growing from 218 K and the intensity increases appreciably with a further lowering in temperature (Figure 8). At 77 K it shows a clear axial-type EPR spectrum, with g_1 = g_2 = 2.19, and g_3 = 2.03. The expected signal at around g = 5 could not be resolved, even at 77 K.

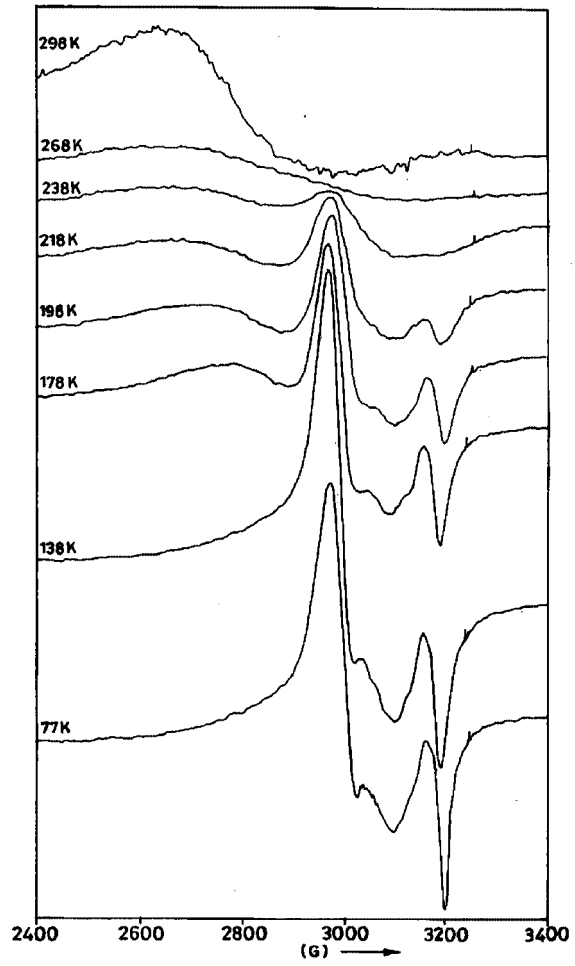

Figure 8. ESR spectra of **16** at variable temperature.

Conclusions

The crystal structures of macrocycles **11** and **12** confirm the formation of 22-membered selenaaza and telluraaza macrocycles incorporating a 1,2-cyclohexane bridge. The replacement of an ethylene bridge with a cyclohexane bridge leads to a significant change in the cavity size. The Se···Se transannular distance for **11** is 5.881 Å, compared with 3.808 Å for **1**, whereas comparison of **2** with **12** indicates a stronger Te···N interaction in **12**. Ligands **3** and **11** both stabilize Co^{II} ion and, as expected, **16** has a longer Co^{II}–Se distance than the Co^{III}–Se bond length. Surprisingly, Co^{II} complex **15** is low-spin whereas **16** is high-spin; both show ESR signals at low temperatures.

Experimental Section

General: Bis(*o*-formylphenyl)selenide,[7a] bis(*o*-formylphenyl)telluride,[6a] ligand **3**, [7b] and $[PdCl_2(C_6H_5CN)_2]$[13] were prepared by reported procedures. Air-sensitive reactions were carried out under an inert atmosphere. Solvents were purified by standard techniques and were freshly distilled prior to use. *trans*-1,2-Diaminocyclohexane was obtained from Aldrich and used as such; 1,3-diaminopropane was reagent grade and was dried and distilled prior to use. Melting points were recorded in capillary tubes and are uncorrected. IR spectra were recorded as KBr pellets on a Perkin–Elmer precisely FTIR spectrometer. Electronic absorption spectra were obtained in $CHCl_3/CH_3CN$ at 25 °C in a 1-cm quartz cuvette with a JASCO V-570 spectrophotometer. ^1H-, ^{13}C-, ^{77}Se-, and ^{125}Te NMR spectra were recorded with a Varian VXR 300S or Varian 400 MHz spectrometer. Chemical shifts cited were referenced to TMS (^1H, ^{13}C) as internal or $SeMe_2$ (^{77}Se) or $TeMe_2$ (^{125}Te) as external standard. Elemental analyses were performed with a Carlo–Erba model 1106 elemental analyzer. ESI mass spectra were recorded at room temperature with a Q-Tof micro (YA-105) mass spectrometer. Variable-temperature magnetic susceptibility data in the temperature range 4–300 K for a polycrystalline sample of **15** and **16** were measured with a Quantum design MPMS squid magnetometer equipped with a closed-cycle cryostat (Air products). $Hg[Co(NCS)_4]$ was used as a standard. Experimental susceptibility data were corrected for diamagnetic contributions. The magnetic moments at various temperatures were calculated by using the expression $2.84(\chi_M T)^{1/2}$. The magnetic susceptibility of **14** was determined at room temperature on a Faraday balance and standardized with mercury tetracyanocobaltate(II) [$\chi = 16.44 \times 10^{-6}\ cm^3\,mol^{-1}$]. The molar susceptibilities were corrected for diamagnetism with the use of Pascal's constants. The effective magnetic moments were calculated by using the expression $\mu_{eff} = 2.84(\chi_M T)^{1/2}$. The ESR measurements for **14**, **15**, and **16** (powder sample) were performed with a Varian model 109CE-line X-band spectrometer fitted with a quartz Dewar for measurements at 77 K and at variable temperature. Cyclic voltammetry experiments were performed with a Scanning Potentiostat EG and G PARC Model 362 instrument, which consists of a one-compartment cell with platinum working and counter electrodes and a standard calomel as reference electrode. Tetrabutylammonium tetrafluoroborate (Aldrich) was used as the supporting electrolyte. All solutions were purged with nitrogen before the CV data were recorded. Measurements were conducted in 0.1 M NBu_4BF_4 in acetonitrile with a sample concentration 0.05 mM. Ferrocene was taken as standard.

Synthesis of Schiff-Base Macrocycle 11: A solution of bis(*o*-formylphenyl)selenide (**9**; 0.313 g, 1 mmol) in acetonitrile (100 mL) was added dropwise to a stirred solution of *trans*-1,2-diaminocyclohexane (0.114 g, 1 mmol) in acetonitrile (200 mL) over a period of five to six hours. The mixture was stirred overnight and the precipitated white powder was filtered off. The solvent was evaporated under reduced pressure and the compound obtained was washed with acetonitrile two or three times. Crystals were grown from a chloroform/hexane mixture. Yield: 0.30 g (76%). M.p. 197–99 °C. ^1H NMR (299.9 MHz, $CDCl_3$, –50 °C): δ = 1.41–2.0 (m, $NCHCH_2CH_2$, 16 H), 3.50 (s, 4 H, $NCHCH_2$), 8.49 (s, 4 H, CH=N), 6.9–7.8 (m, 16 H, Ar-*H*) ppm. ^{13}C NMR (100.5 MHz, $CDCl_3$, room temp.): δ = 23.6, 31.8, 73.7, 126.9, 130.1, 130.1, 135.2, 136.9, 161.1 ppm; all peaks are broad). ^{13}C NMR (75.4 MHz, $CDCl_3$, –50 °C): δ = 20.5, 24.1, 26.3, 32.5, 71.8, 75.2, 124.6, 127.9, 129.6 (t), 130.4, 131.7, 133.4, 135.1, 136.5, 136.8, 138.8, 160.1, 161.6 ppm. ^{77}Se NMR (57.2 MHz, $CDCl_3$): δ = 404 ppm. IR (KBr): $\tilde{\nu}$ = 1641 cm^{-1} ν(C=N). UV/Vis (CH_2Cl_2): λ_{max} (ε, $M^{-1}\,cm^{-1}$) = 240 (12938), 332 nm (1869). ESI-MS ($CHCl_3$): *m*/*z* (%) = 737 (100) $[M]^+$. $C_{40}H_{40}N_4Se_2$: calcd. C 65.40, H 5.48, N 7.62; found C 65.20, H 5.51, N 7.51.

Synthesis of Schiff-Base Macrocycle 12: A solution of bis(*o*-formylphenyl)telluride (**10**; 0.398 g, 1 mmol) in acetonitrile was added dropwise to a stirred solution of *trans*-1,2-diaminocyclohexane (0.114 g, 1 mmol) in acetonitrile (200 mL) over a period of five to six hours. The mixture was stirred overnight and the precipitated white powder was filtered off. The solvent was evaporated under reduced pressure and the compound obtained was washed with acetonitrile two or three times. Yield: 0.28 g (57%). M.p. 200–202 °C. ^1H NMR (399.99 MHz, $CDCl_3$): δ = 1.45–1.90 (m, 16 H, $NCHCH_2CH_2$), 3.63 (s, 4 H, $NCHCH_2$), 7.09–8.01 (m, Ar-H, 16 H), 8.53 (s, 4 H, N=CH) ppm. ^{13}C NMR (100.5 MHz, $CDCl_3$): δ = 58.1, 126.3, 130.1, 132.9, 138.5, 144.5, 166.7, 167.3 ppm. ^{125}Te NMR (94.78 MHz, $CDCl_3$): δ = 581 ppm. IR (KBr): $\tilde{\nu}$ = 1637 cm^{-1} ν(C=N). UV/Vis (CH_2Cl_2): λ_{max} (ε, $M^{-1}\,cm^{-1}$) = 368 (16676), 332 nm (2541). ESI-MS ($CHCl_3$): *m*/*z* (%) = 832 (100) $[M]^+$. $C_{40}H_{40}N_4Te_2$: calcd. C 57.74, H 4.84, N 6.73; found C 57.88, H 5.20, N 7.18.

Synthesis of Reduced Macrocycle 13: An excess of $NaBH_4$ was added, in small portions, to a suspension of **11** (0.734 g, 1 mmol) in ethanol, and the reaction mixture was stirred for 4 h at room temperature, after which time it was heated at reflux for 3–4 h. The excess of ethanol was removed under reduced pressure. Water was added to the residue and the product was extracted with chloroform and kept over sodium sulfate. It was filtered and the solvents evaporated to dryness. The residue was used for characterization. Colour: white. Yield: 0.49 g (66%). M.p. 240–242 °C. ^1H NMR (399.99 MHz, $CDCl_3$): δ = 1.0 (br. s, 4 H, CH_2NH), 1.2 (m, 8 H, $CHCH_2CH_2$), 1.7 (m, 8 H, $CHCH_2CH_2$), 2.3 (m, 4 H, NCH), 3.9 (dd, *J* = 13.4 Hz, 8 H, NCH_2), 6.95–7.25 (m, 16 H) ppm. ^{13}C NMR (75.43 MHz, $CDCl_3$): δ = 30.1, 50.4, 24.4, 58.2, 126.2, 127.6, 129.1, 129.9, 130.9, 140.8 ppm. ^{77}Se NMR (57.2 MHz, $CDCl_3$): δ = 340 ppm. IR (KBr): $\tilde{\nu}$ = 3300, 3277, 3165, 3053, 1460 (N-H bending). ESI-MS: *m*/*z* = 743 $[M]^+$. $C_{40}H_{48}N_4Se_2$: calcd. C 64.69, H 6.51, N 7.54; found C 64.52, H 6.93, N 7.29.

Synthesis of Complex 14: Schiff-base ligand **11** (0.245 g, 0.33 mmol) was added to a two-necked, round-bottomed flask along with methanol (20 mL). After stirring for some time, $NiCl_2{\cdot}6H_2O$ (0.08 g, 0.33 mmol) was added and the mixture refluxed for one hour, the color of the reaction mixture changing to a clear reddish-brown. An excess of ammonium hexafluorophosphate was then added. The reddish-brown precipitate formed was filtered off and washed with methanol. Complex **14** was recrystallized as reddish-brown needles by slow diffusion of diethyl ether into a MeCN solution. Yield: 0.30 g (84%). M.p. 250–252 °C (dec.). IR (KBr): $\tilde{\nu}$ = 2935, 1627, 1291, 848, 766, 586 cm^{-1}. UV/Vis (MeCN): λ_{max} (ε, $M^{-1}\,cm^{-1}$) = 218 (12752), 348 (613), 450 (123), 850 nm (50). μ_{eff} = 2.5 μ_B. ESI-MS: *m*/*z* (%) = 793 (100) $[M - 2PF_6]^+$, 939 (50) $[M - PF_6]^+$. $C_{40}H_{40}F_{12}N_4NiP_2Se_2$: calcd. C 44.35, H 3.72, N 5.17; found C 44.59, H 3.48, N 5.25.

Synthesis of Complex 15: $Co(ClO_4)_2{\cdot}6H_2O$ (0.12 g, 0.33 mmol) was added to a suspension of ligand **11** (0.25 g, 0.33 mmol) in acetonitrile. The color of the reaction mixture changed from light brown to dark brown, and after stirring for 4–5 h a clear brown solution had formed. The reaction mixture was stirred overnight and was then filtered and evaporated to 15 mL. It was kept as such for crystallization, which produced a black, crystalline compound. Yield: 0.23 g (68%). IR (KBr): $\tilde{\nu}$ = 1617 cm^{-1} ν(C=N), 1591, 1092, 624. UV/Vis (CH_3CN): λ_{max} (ε, $M^{-1}\,cm^{-1}$) = 222 (15162), 356 (1487), 546 nm (218). ESI-MS: *m*/*z* (%) = 795 (50) $[M - 2ClO_4]^+$, 894 (20)

$[M - ClO_4]^+$. $C_{40}H_{40}Cl_2CoN_4O_8Se_2$: calcd. C 48.41, H 4.06, N 5.64; found C 48.29, H 4.14, N 5.94.

Synthesis of Complex 16: $Co(ClO_4)_2 \cdot 6H_2O$ (0.10 g, 0.33 mmol) was added to a suspension of ligand **3** (0.22 g, 0.33 mmol) in acetonitrile (60 mL) and stirred for overnight. The solution was then filtered and evaporated to 20 mL. Diethyl ether was added to this solution to induce crystallization. The brown, crystalline product that separated was used for characterization. Yield: 0.20 g (65%). UV/Vis (CH_3CN): λ_{max} (ε, $M^{-1}cm^{-1}$) = 224 (18141), 354 (1734), 546 nm (285). ESI-MS: *m/z* (%) = 814 (50) $[M - 2ClO_4]^+$. $C_{34}H_{32}Cl_2CoN_4O_8Se_2$: calcd. C 44.76, H 3.53, N 6.14; found C 44.58, H 3.12, N 6.24.

Synthesis of Complex 17: $[PdCl_2(C_6H_5CN)_2]$ (0.13 g, 0.33 mmol) in dichloromethane (10 mL) was added dropwise to a chloroform (10 mL) solution of **12** (0.33 mmol, 0.28 g). On stirring for 2 h, a yellow solution formed. After stirring for a further 2 h the yellow solution was evaporated and the residue was dissolved in methanol (5 mL), to which an excess of NH_4PF_6 was added. The yellow product formed was washed with diethyl ether and recrystallized from acetonitrile. Yield: 0.24 g (58%). M.p. 260–62 °C (dec.). ^1H NMR (399.99 MHz, CD_3CN): δ = 1.4–2.5 (m, 16 H, NCHCH_2CH_2), 3.6 (d, J = 8.9 Hz, 2 H, NCHCH_2), 4.0 (d, J = 3.9 Hz, 2 H, NCHCH_2), 7.0 (d, J = 7.8 Hz, 2 H), 7.32 (t, J = 7.8 Hz, 2 H), 7.4 (m, 4 H), 7.55 (m, 4 H), 7.92 (d, J = 7.4 Hz, 2 H), 8.2 (d, J = 7.4 Hz, 2 H), 8.5 (s, 2 H, CH=N), 9.0 (s, 2 H, CH=N) ppm. ^{13}C NMR (100.5 MHz, CD_3CN): δ = 25.4, 25.6, 31.9, 33.6, 68.5, 75.3, 119.4, 122.2, 132.1, 132.8, 134.1, 135.2, 135.3, 135.8, 137.2, 138.9, 139.2, 140.6, 162.4, 168.9 ppm. ^{125}Te NMR (94.87 MHz, CD_3CN): δ = 751 ppm. UV/Vis (CH_3CN): λ_{max} (ε, $M^{-1}cm^{-1}$) = 218 (17794), 304 (5044), 394 nm (1583). ESI-MS (CH_3CN): *m/z* (%) = 939 (20) $[M - 2PF_6]^+$, 957 (70) $[M - 2PF_6 + H_2O]^+$, 1085 (50) $[M - PF_6]^+$.

X-ray Crystallographic Studies: The diffraction measurements for the ligands as well as the complexes were performed at room temperature with a "Bruker P4" diffractometer with graphite-monochromated Mo-K_α radiation (λ = 0.71073 Å). The data were corrected for Lorentz, polarization, and absorption effects The structures were determined by routine heavy-atom and Fourier methods by using SHELXS 97[14] and refined by full-matrix least-squares with the non-hydrogen atoms anisotropic and hydrogen with fixed isotropic thermal parameters of 0.07 Å by means of the SHELXL 97[15] program. The hydrogens were partially located from difference electron-density maps and the rest were fixed at predetermined positions. Scattering factors were from common sources.[16] Some details of data collection and refinement are given in Tables 5 and 6.

Table 5. Crystallographic data for compound **11** and **12**.

	11	**12**
Empirical formula	$C_{20}H_{20}N_2Se$	$C_{41}H_{42}Cl_2N_4Te_2$
Fw	367.34	916.89
Crystal system	triclinic	triclinic
Space group	$P\bar{1}$	$P\bar{1}$
a [Å]	11.4037(11)	11.2692(9)
b [Å]	11.8184(12)	12.8612(11)
c [Å]	14.6835(14)	15.2439(12)
α [°]	73.693(2)	66.6600(10)
β [°]	87.145(3)	75.1630(10)
γ [°]	64.196(2)	73.4570(10)
V [Å^3]	1703.9(3)	1918.7(3)
Z	4	2
$D_{calcd.}$ [mg m^{-3}]	1.432	1.587
Temp [K]	103(2)	103(2)
θ range [°]	2.10–27.84	1.86–28.33
Abs. coeff. [mm^{-1}]	2.205	1.694
Final $R(F)$ $[I > 2\sigma(I)]$[a]	0.0448	0.0278
$wR(F^2)$ indices $[I > 2\sigma(I)]$	0.1177	0.0629
Data/restraints/parameters	7181/0/416	8969/0/443
Goodness of fit on F^2	1.086	1.046

[a] Definitions: $R(F_o) = \sum||F_o| - |F_c||/\sum|F_o|$ and $wR(F_o^2) = \{\sum[w(F_o^2 - F_c^2)^2]/\sum[w(F_c^2)^2]\}^{1/2}$.

Table 6. Crystallographic data for Compound **14** and **16**.

	14	**16**
Empirical formula	$C_{40}H_{42}F_{12}N_4NiP_2Se_2$	$C_{34}H_{32}Cl_2CoN_4O_8Se_2$
Fw	1085.35	912.39
Crystal system	hexagonal	monoclinic
Space group	$P6_1$	C_2
a [Å]	17.0747(16)	17.160(2)
b [Å]	17.0747(16)	10.9660(14)
c [Å]	29.958(4)	9.4941(12)
α [°]	90	90
β [°]	90	104.351(2)
γ [°]	120	90
V [Å^3]	7564.0(14)	1730.8(4)
Z	6	2
$D_{calcd.}$ [mg m^{-3}]	1.430	1.751
Temp [K]	293(2)	293(2)
λ [Å]	0.71073	0.71073
θ range [°]	1.54–28.93	2.21–28.32
Abs. coeff. [mm^{-1}]	1.967	2.812
Obsd. reflections $[I > 2\sigma(I)]$	57207	6330
Final $R(F)$ $[I > 2\sigma(I)]$[a]	0.0545	R_1 = 0.0321
$wR(F^2)$ indices $[I > 2\sigma(I)]$	0.1486	wR_2 = 0.0778
Data/restraints/parameters	12299/1/550	3873/1/232
Goodness of fit on F^2	1.030	1.066

[a] Definitions: $R(F_o) = \sum||F_o| - |F_c||/\sum|F_o|$ and $wR(F_o^2) = \{\sum[w(F_o^2 - F_c^2)^2]/\sum[w(F_c^2)^2]\}^{1/2}$.

CCDC-604888 (**11**), -604889 (**12**), -604890 (**14**) and -604891 (**16**) contain the supplementary crystallographic data for this paper. These data can be obtained free of charge from The Cambridge Crystallographic Data Centre via www.ccdc.cam.ac.uk/data_request/cif.

Acknowledgments

We are grateful to the Department of Science and Technology (DST), New Delhi, and the Council of Science and Industrial Research (CSIR), New Delhi, for funding this work. Additional help from the Sophisticated Analytical Instrumentation Facility (SAIF), Indian Institute of Technology (IIT), Bombay, for 300 MHz NMR spectroscopy is also acknowledged. We are grateful to Prof. G. K. Lahiri for useful discussions regarding the magnetic susceptibility data and ESR. Prof. G. Mugesh (IISC Bangalore) and Prof. A. K. Nigam (TIFR, Bombay) are gratefully acknowledged for their help in recording the magnetic susceptibility data.

[1] a) C. Bornet, R. Amardeil, P. Meunier, J. C. Daran, *J. Chem. Soc., Dalton Trans.* **1999**, 1039; b) J. L. Li, J. B. Meng, Y. M. Wang, J. T. Wang, T. Matsuura, *J. Chem. Soc., Perkin Trans. 1* **2001**, 1140; c) M. Iwaoka, S. Tomoda, *J. Am. Chem. Soc.* **1994**, *116*, 4463; d) A. Mazouz, J. Bodiguel, P. Meunier, B. Gautheron, *Phosphorus Sulfur Silicon Relat. Elem.* **1991**, *61*, 247; e) A. Mazouz, P. Meunier, M. M. Kubicki, B. Hanquet, R. Amardeil, C. Bornet, A. Zahidi, *J. Chem. Soc., Dalton Trans.* **1997**, 1043; f) X. Zeng, X. Han, L. Chen, Q. Li, F. Xu, X. He, Z. Zhang, *Tetrahedron Lett.* **2001**, *43*, 131.

[2] a) K. Kobayashi, H. Izawa, K. Yamaguchi, E. Horn, N. Furukawa, *Chem. Commun.* **2001**, 1428; b) M. J. Hesford, W. Levason, M. L. Matthews, G. Reid, *Dalton Trans.* **2003**, 2852.
[3] a) R. J. Batchelor, F. W. B. Einstein, I. D. Gay, J. H. Gu, S. Mehta, B. M. Pinto, X. M. Zhou, *Inorg. Chem.* **2000**, *39*, 2558; b) M. J. Hesford, W. Levason, M. L. Matthews, S. D. Orchard, G. Reid, *Dalton Trans.* **2003**, 2434.
[4] S. Muralidharan, M. Hojjatie, M. Firestone, H. Freiser, *J. Org. Chem.* **1989**, *54*, 393.
[5] R. Bhula, A. P. Arnold, G. J. Gainsford, W. G. Jackson, *Chem. Commun.* **1996**, 143.
[6] a) S. C. Menon, H. B. Singh, R. P. Patel, S. K. Kulshereshtha, *J. Chem. Soc., Dalton Trans.* **1996**, 1203; b) S. C. Menon, A. Panda, H. B. Singh, R. J. Butcher, *Chem. Commun.* **2000**, 143; c) S. C. Menon, A. Panda, H. B. Singh, R. P. Patel, S. K. Kulshereshtha, W. L. Darby, R. J. Butcher, *J. Organomet. Chem.* **2004**, *689*, 1452.
[7] a) A. Panda, S. C. Menon, H. B. Singh, R. J. Butcher, *J. Organomet. Chem.* **2001**, *623*, 87; b) A. Panda, S. C. Menon, H. B. Singh, C. P. Morley, R. Bachman, T. M. Cocker, R. J. Butcher, *Eur. J. Inorg. Chem.* **2005**, *6*, 1114; c) S. Panda, H. B. Singh, R. J. Butcher, *Chem. Commun.* **2004**, 322; d) S. Panda, H. B. Singh, R. J. Butcher, *Inorg. Chem.* **2004**, *43*, 8532; e) S. Panda, H. B. Singh, R. J. Butcher, *Eur. J. Inorg. Chem.* **2006**, *7*, 172.
[8] a) W. Levason, J. J. Quirk, G. Reid, *J. Chem. Soc., Dalton Trans.* **1996**, 3713.
[9] F. A. Cotton, G. Wilkinson *Advanced Inorganic Chemistry, A Comprehensive Text*, Wiley Eastern Limited, 3rd ed., India, **1993**, p. 894.
[10] a) M. Schröder, *Encyclopedia of Inorganic Chemistry* (Ed.: R. B. King), Wiley, New York, **1994**, vol. 5, p. 2395; b) L. Sacconi, F. Mani, A. Benicini, *Comprehensive Coordination Chemistry* (Eds.: G. Wilkinson, R. D. Gillard, J. A. McCleverty), Pergamon, **1987**, vol. 5, p. 55.
[11] P. B. Ayscough, *Electron Spin Resonance Chemistry*, Methuen and Co. Ltd., **1967**.
[12] J. A. Weil, J. R. Bolton, E. Wertz, *Electron Spin Resonance, Elementary Theory and Practical Applications*, 2nd ed., Wiley, New York, **1994**.
[13] J. R. Doyle, P. E. Slade, H. B. Jonassen, *Inorg. Synth.* **1960**, *6*, 218.
[14] G. M. Sheldrick, SHELXS 97, *Program for the Solution of Crystal Structures*, University of Göttingen, Germany, **1990**.
[15] G. M. Sheldrick, SHELXL 97, *Program for Refining Crystal Structures*, University of Göttingen, Germany, **1997**.
[16] D. T Cromer; J. T. Waber *International Tables for X-ray Crystallography*, Kynoch Press, Birmingham, **1974**, vol. IV, p. 99 and p. 149.

Received: May 29, 2006
Published Online: October 27, 2006

